Development 139, 525-536 (2012) doi:10.1242/dev.066522

Midbrain-hindbrain boundary patterning and morphogenesis are regulated by diverse grainy head-like 2-dependent pathways

Sebastian Dworkin[1], Charbel Darido[1], Smitha R. Georgy[1], Tomasz Wilanowski[1,*], Seema Srivastava[1], Felix Ellett[2], Luke Pase[2], Yanchao Han[3], Anming Meng[3], Joan K. Heath[4], Graham J. Lieschke[2] and Stephen M. Jane[1,5,‡]

SUMMARY

The isthmic organiser located at the midbrain-hindbrain boundary (MHB) is the crucial developmental signalling centre responsible for patterning mesencephalic and metencephalic regions of the vertebrate brain. Formation and maintenance of the MHB is characterised by a hierarchical program of gene expression initiated by fibroblast growth factor 8 (*Fgf8*), coupled with cellular morphogenesis, culminating in the formation of the tectal-isthmo-cerebellar structures. Here, we show in zebrafish that one orthologue of the transcription factor grainy head-like 2 (*Grhl2*), zebrafish *grhl2b* plays a central role in both MHB maintenance and folding by regulating two distinct, non-linear pathways. Loss of *grhl2b* expression induces neural apoptosis and extinction of MHB markers, which are rescued by re-expression of *engrailed 2a* (*eng2a*), an evolutionarily conserved target of the Grhl family. Co-injection of sub-phenotypic doses of *grhl2b* and *eng2a* morpholinos reproduces the apoptosis and MHB marker loss, but fails to substantially disrupt formation of the isthmic constriction. By contrast, a novel direct *grhl2b* target, *spec1*, identified by phylogenetic analysis and confirmed by ChIP, functionally cooperates with *grhl2b* to induce MHB morphogenesis, but plays no role in apoptosis or maintenance of MHB markers. Collectively, these data show that MHB maintenance and morphogenesis are dissociable events regulated by *grhl2b* through diverse transcriptional targets.

KEY WORDS: Midbrain-hindbrain boundary, Morphogenesis, Patterning, Grainy head-like 2, Engrailed, Fgf8, Zebrafish

INTRODUCTION

The grainy head-like (Grhl) family of transcription factors are important regulators of neural development in diverse species. In *Drosophila*, *grainy head* (*grh*) is a key determinant of neuroblast specification, proliferation and apoptosis (Bray and Kafatos, 1991; Uv et al., 1997; Almeida and Bray, 2005; Cenci and Gould, 2005; Maurange et al., 2008), whereas, in mammals, the *Grhl* homologues functionally demarcate distinct regions of neural tube closure, failure of which leads to neural tube defects (NTD) (Ting et al., 2003; Rifat et al., 2010). Mice lacking the *Grhl3* gene survive to birth and exhibit thoraco-lumbo-sacral spina bifida, and, rarely, exencephaly (Ting et al., 2003). By contrast, *Grhl2*-null mice die at embryonic day (E) 11.5, and display severe cranial neurulation defects, including a fully-penetrant 'split-face' malformation associated with cranioschisis, and also an open posterior neuropore (Rifat et al., 2010). The molecular bases for the profound defects in the *Grhl2*-null embryos are yet to be elucidated.

Clues to the roles of the mammalian *Grhl* members in both neural and non-neural developmental processes have emerged from studies of *grh* function in *Drosophila* embryogenesis. Of the known homologs of established *grh* target genes that have been implicated in vertebrate neural development, *engrailed1* and *engrailed2* (*En1, En2*), homologs of the segment polarity gene *engrailed*, represent potential candidate downstream effectors of the *Grhl2* gene (Attardi and Tjian, 1993). The vertebrate engrailed genes are important for the molecular and cellular control of mesencephalon and metencephalon development (Joyner et al., 1991; Wurst et al., 1994; Joyner, 1996), contributing to both the establishment and maintenance of the midbrain/hindbrain boundary (MHB) (Hidalgo-Sanchez et al., 2005; Sato et al., 2004). The biochemical pathways mediating this are highly conserved phylogenetically, with the *Drosophila engrailed* gene capable of substituting for mouse *En1* function in the mid-hindbrain (Hanks et al., 1998). The DNA consensus binding site of *grh* and the mammalian *Grhl* factors (AACCGGTT) is absolutely conserved across 700 million years of evolution (Wilanowski et al., 2008; Caddy et al., 2010), and we have previously shown that *En1* is a putative mammalian *Grhl* target (Wilanowski et al., 2002). To explore the role of the *Grhl2* gene in vertebrate neurulation, and to determine the functional relationship between *Grhl2* and the engrailed genes, we elected to use the genetically tractable zebrafish model, with the aim of defining conserved developmental pathways.

MATERIALS AND METHODS

Cloning of zebrafish grhl2b

Zebrafish *grhl2b* was cloned from 18-24 hpf wild-type AB-strain fish cDNA by PCR amplification using Phusion polymerase (Finnzymes, Espoo, Finland), to minimise the chance of capricious mutations. Full-

[1]Department of Medicine, Monash University Central Clinical School, Prahran VIC 3181, Australia. [2]Australian Regenerative Medicine Institute, Monash University, Clayton, Victoria, 3168, Australia. [3]Developmental Genetics Laboratory of Tsinghua University, School of Life Sciences, Tsinghua University, Beijing 100084, China. [4]Colon Molecular and Cell Biology Laboratory, Ludwig Institute for Cancer Research, Royal Melbourne Hospital, Parkville, Victoria 3050, Australia. [5]Alfred Hospital, Prahran VIC 3181, Australia.

*Present address: Laboratory of Signal Transduction, Nencki Institute of Experimental Biology 02-093 Warsaw, Poland
‡Author for correspondence (stephen.jane@monash.edu)

Accepted 22 November 2011

length PCR products were cloned into pCRII-TOPO (Invitrogen, Carlsbad, CA), and confirmed by sequencing. Verified coding DNAs were sub-cloned into pCS2+ (Turner and Weintraub, 1994) to generate the vector pCS2+*grhl2b*, and used for subsequent transcription of CpG-capped mRNA using the mMESSAGE mMACHINE kit (Ambion, Austin, TX).

Morpholino oligonucleotides (MO) and zebrafish micro-injection

Zebrafish embryos were micro-injected at the one- to two-cell stage with a bolus of approximately 2 nl. Dose-titration experiments were performed for all mRNAs/MO to determine optimum experimental dosages (supplementary material Table S1; data not shown). Murine Grhl2 and zebrafish eng2a mRNAs were injected at a concentration of 75-125 pg/bolus, whereas MO for *grhl2b* were routinely injected at concentrations of approximately 200 mM (ATG-blocking) and 250 mM (splice blocking and mismatch control). MOs targeting *spec1* were both injected at a concentration of 250 mM. The ATG-blocking MO targeting *grhl2a* was injected at a concentration of 200 mM. The sequences for ATG and splice blocking and control MO for *grhl2b*, *grhl2a* and *spec1* are listed in supplementary material Table S3. The sequences and doses of the ATG-blocking MOs targeting *eng2a* or *fgf8* were as previously published (Araki and Brand, 2001; Scholpp and Brand, 2001). The sub-phenotypic doses of the *grhl2b*, *eng2a* and *fgf8* MO were 100 mM, and the *spec1* dose was 125 mM. Zebrafish protocols were pre-approved by the Walter and Eliza Hall Institute Animal Ethics Committee.

In situ hybridisation and imaging

Two independent *grhl2b* probes were cloned from 24 hpf AB-strain zebrafish [corresponding to nucleotides 219-759 and 1329-1779 of *grhl2b* (NM_001083072)]. Both probes were verified by sequencing before use and showed an identical expression pattern. All in situ hybridisation and imaging procedures were conducted as reported previously (Dworkin et al., 2007).

Reporter gene assays

A 3 kb fragment of the zebrafish *eng2a* promoter corresponding to positions –3029 to –29 relative to the transcriptional start site was amplified by PCR from wild-type AB 24 hpf genomic DNA and cloned into the pGL3basic-Luciferase vector to generate the vector pGL3*eng2a*PROM. Regulation of the *eng2a* promoter was assessed in vivo using the dual Luciferase reporter assay (Promega, Fitschburg, WI), following methods previously reported (Alcaraz-Perez et al., 2008).

Generation of MO-resistant *grhl2b*

The 5′ region of pCS2+*grhl2b* mRNA was amplified by PCR to generate a 7 bp mutation within the MO-recognition site without altering the amino acids synthesised. Making use of a 5′*Eco*RI site introduced into the product by the forward primer, and an existing *Ale*I site towards the 3′ end of the amplicon, the PCR product was digested with *Eco*RI and *Ale*I, and cloned into similarly digested pCS2+*grhl2b*, resulting in a change from **ATG**TCACAGGAGACAGACAGTAAG to **ATG**TCtCAaGAaACtGAt-AGcAAa. The presence of the new 7 bp mismatch MO-binding region was verified by sequencing.

Cell death analysis assays

TUNEL staining to detect apoptosis was performed using the TMR Red In Situ Cell Death Detection Kit (Roche, Basel, Switzerland) according to the manufacturer's instructions. Embryos were imaged by fluorescence microscopy on an Olympus FV1000 single-photon confocal microscope.

Laser capture microdissection and mRNA amplification

Paraformaldehyde-fixed embryos (11-12 hpf) were sequentially embedded in agarose and paraffin and 8 mm sections were cut onto PEN membrane slides. The sections were stained with the Histogene laser capture microdissection staining kit immediately prior to laser capture microdissection. The MHB region from four embryos was microdissected using a Veritas microdissection instrument (Arcturus) according to standard protocols and the tissues were captured onto Capsure HS laser capture microdissection caps. RNA extraction and amplification were performed according to the manufacturers' instructions (Arcturus).

Quantitative RT-PCR

All Q-RT-PCR analysis was performed using GoTaq SyBR Green mastermix (Promega) and a Roche LC480 LightCycler (Roche, Basel, CH). Data were collated from a minimum of three samples per group, and expression levels were normalised to the gene encoding the housekeeping protein β-actin.

Generation of c-terminal FLAG fusion to *grhl2b*

The 3′ coding sequence of pCS2+*grhl2b* was mutagenised using the QuikChange site-directed mutagenesis kit (Stratagene, La Jolla, CA), resulting in a single minor amino acid change of isoleucine to leucine at codon 600 (immediately prior to the terminal stop codon), thereby introducing a *Sac*I site (GAAATA to GAGCTC). Complementary oligonucleotides consisting of sequence coding for a 5′ *Sac*I site-FLAG-tag-stop codon-3′ *Xho*I site were generated and annealed. Making use of the novel *Sac*I site in pCS2+*grhl2b* and an existing *Xho*I site at position 2147, *Sac*I/*Xho*I double digestion facilitated cloning of the FLAG-tag into pCS2+*grhl2b* to generate the vector pCS2+*grhl2b*-FLAG. Following sequencing to confirm in-frame fusion of the FLAG-tag, pCS2+*grhl2b*-FLAG was transfected into HEK-293T cells and FLAG-tagged *grhl2b* protein was detected by western blotting using monoclonal anti-FLAG M2 antibody (Sigma-Aldrich, St Louis, MO) and standard methods.

Chromatin immunoprecipitation (ChIP) assay

ChIP assays were performed using the 'microChIP' protocol (Dahl and Collas, 2008), optimised for low starting cell number. Chromatin was derived from 50,000-100,000 cells, extracted from five to eight individual (de-yolked) zebrafish embryos per group. *grhl2b*-FLAG was immunoprecipitated using the anti-FLAG M2 antibody; negative controls were performed using anti-mouse IgG antibody (Sigma-Aldrich). As an additional specificity control, ChIP assays using anti-FLAG antibody were performed on zebrafish overexpressing non-FLAG-tagged *grhl2b* mRNA. Specific oligonucleotides flanking the predicted *grhl2b*-binding sites in the promoters of both *eng2a* and *spec1* were used to amplify the enriched loci; primers ~3 kb upstream of the predicted promoter binding sites and also ~1 kb downstream of the transcription start site (within the coding regions) for both *eng2a* and *spec1* were used as negative controls for binding.

RESULTS

Characterisation of the zebrafish *grhl2* family

Previous work had identified two orthologues of mammalian *Grhl2* in zebrafish – termed *zgrhl2a* and *zgrhl2b*, respectively (Janicke et al., 2010). Our analyses suggest that, based on homology with mammalian *Grhl2*, a previously deposited sequence (termed 'Danio rerio hypothetical LOC558268, transcript variant 2', GenBank Accession Number XM_701793) was more likely to be the correct full-length isoform of *zgrhl2b*. This sequence included 47 additional amino acids at the N terminus, but was otherwise identical with the sequence deposited as '*zgrhl2b*' (GenBank Accession Number NM_001083072). Of these additional 47 amino acids, 36 were identical to both human and mouse *Grhl2*, and 34/47 nucleotides were also conserved in *zgrhl2a*. These homology analyses are shown in supplementary material Fig. S1A,B. Further confirmation of this N-terminal exon has been recently provided by others using 5′ RACE (Han et al., 2011). As *grhl2b* exhibits a higher degree of homology to mammalian *Grhl2*, our initial studies focused on characterising this orthologue.

Loss of *grhl2b* induces MHB and otic vesicle defects

The early expression patterns of *grhl2b* in the developing fish are shown in supplementary material Fig. S1C-G. In our initial functional experiments, an ATG-directed antisense MO that blocked *grhl2b* mRNA translation was used to examine the developmental consequences of *grhl2b* loss of function. Morphants

lacking *grhl2b* developed normally until ~21 hours post fertilisation (hpf), at which time the MHB region failed to undergo its characteristic horseshoe-shaped folding. By 24 hpf, this phenotype became more pronounced, and was accompanied by defective ventricle formation, and marked neural cell death (arrowed) in the midbrain and hindbrain regions (Fig. 1A,B, inset). The neural cell death was shown to be apoptotic by TUNEL assay (Fig. 1C,D). The severity of the phenotype correlated with the concentration of the *grhl2b*-MO injected (supplementary material Table S1), and an identical phenotype was observed utilising an exon 1/intron 1 (E1/I1) splice-blocking MO (supplementary material Fig. S2A-C). Some apoptosis was also visible in the trunk and tail with this MO (supplementary material Fig. S2D).

Recent studies of a mutant zebrafish line generated by Tol2 transposon-based gene trapping of an EGFP reporter into the first intron of the *grhl2b* gene demonstrated otic vesicle defects (Han et al., 2011). We confirmed that otolith formation was also disrupted in our ATG-blocking MO-injected morphants (supplementary material Fig. S3A), and that this defect could be rescued by injection of murine *Grhl2* mRNA (supplementary material Fig. S4B). Otic expression of both *claudin b* and *epcam* was lost in our morphants, phenocopying the expression changes observed in the *grhl2b* mutant line (supplementary material Fig. S3C-F) (Han et al., 2011). However, no MHB defects were noted in this line, which we attribute to persistence of tissue-specific expression of *grhl2b* in the MHB region or, alternatively, to the presence of an alternate spliced isoform of *grhl2b* in the MHB (supplementary material Fig. S3G,H), a frequent event in gene trapping-based mutants (Clark et al., 2011).

Ontogeny of the MHB occurs in three stages: *Fgf8/Wnt1*-mediated positioning of the MHB boundary at the interface of *otx2* (midbrain) and *gbx2* (hindbrain) expression in the neural plate (~6 hpf) (*otx2/gbx1* interface in zebrafish) (Rhinn et al., 2009); induction of the MHB differentiation program, characterised by

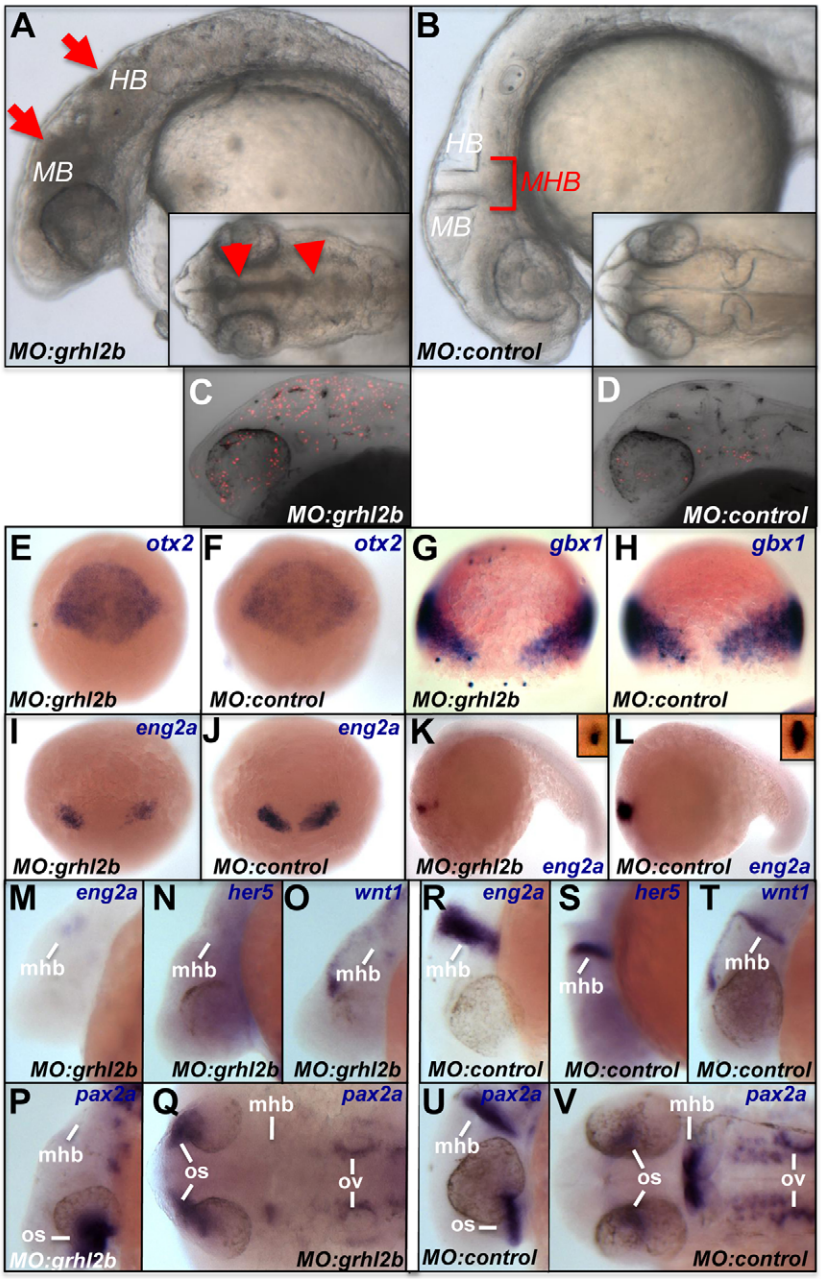

Fig. 1. Loss of function of *grhl2b* leads to severe defects in the MHB region. (**A**,**B**) Embryos injected with control or *grhl2b* ATG-blocking MO. Lateral views with dorsal views in the insets. MB, midbrain; HB, hindbrain; apoptosis and folding defects are indicated by arrows and arrowheads. (**C**,**D**) Apoptosis is increased in *grhl2b* morphants (MO:*grhl2b*) compared with controls. (**E-H**) Positioning of either the midbrain (*otx2*) or hindbrain (*gbx1*) territories within the neural plate in *grhl2b* morphants compared with controls. (**I-L**) Expression of *eng2a* in *grhl2b* morphants and controls from the onset of MHB formation. (**M-V**) Expression of MHB patterning genes (*eng2a*, *her5, wnt1* and *pax2a*) at 26 hpf in *grhl2b* morphants and controls. mhb, midbrain-hindbrain boundary; os, optic stalk; ov, otic vesicles.

expression of genes including *pax2a*, *wnt1*, *her5* and *eng2a* (~9 hpf); and finally, maintenance of the MHB involving both feedback regulation and transcriptional interdependence of these genes (~16-28 hpf) (Lun and Brand, 1998; Liu and Joyner, 2001; Martinez, 2001; Rhinn and Brand, 2001; Wurst and Bally-Cuif, 2001; Chi et al., 2003; Hidalgo-Sanchez et al., 2005). To analyse MHB development, we examined the expression of these crucial genes in the *grhl2b* loss-of-function and control MO-injected embryos. To ensure precise temporal comparison of gene expression, controls and *grhl2b* morphants were developmentally staged by expression of *pax2a*, which is sequentially expressed in the MHB, pronephric mesoderm and otic vesicles between 9 and 10 hpf (Thisse and Thisse, 2004) (data not shown). Neither *otx2* nor *gbx1* expression was altered in *grhl2b* morphants during the positioning/induction phases of MHB formation (Fig. 1E-H), suggesting that *grhl2b* does not play a role in regionalising the presumptive neural territories within the neural plate, or in positioning the midbrain/hindbrain at the junction of these regions. At the onset of the MHB induction signalling cascade, expression of the key patterning genes *pax2a*, *wnt1* and *her5* was unchanged between *grhl2b* morphants and controls, whereas *eng2a* expression was markedly reduced in the *grhl2b*-MO-injected embryos (Fig. 1I,J; supplementary material Fig. S4A-C′). This exclusive downregulation of *eng2a* was also apparent during the early stages of neural tube morphogenesis (14 hpf) and after morphological establishment of the MHB (23 hpf; Fig. 1K,L; data not shown). Expression of other MHB markers was not altered at these time points (supplementary material Fig. S4D-E′; data not shown). However, by 26 hpf, expression of MHB markers was substantially reduced or lost in 56/79 embryos examined [*eng2a* (22/27), *wnt1* (8/11), *pax2a* (21/32) and *her5* (5/9); supplementary material Table S1], indicating that *grhl2b* impacts on MHB maintenance at both structural and molecular levels (Fig. 1M-V). Interestingly, *pax2a* expression was also lost in the ventral hindbrain neurons of *grhl2b* morphants (Fig. 1Q), although whether this is due to direct regulation, loss of *eng2a*-dependent feedback loops or as a secondary consequence of increased apoptosis/decreased organiser fidelity remains to be determined. As specific staining of *pax2a* was observed both anteriorly (in the optic stalk) and posteriorly (in the otic vesicles) in *grhl2b*-morphants (Fig. 1P,Q), *grhl2b* does not appear to have a role in regulating patterning or gene expression at neural regions outside the brain. Consistent with this, expression of several well characterised patterning and specification genes, including *fgf8*, *dlx3* (margin and neural plate), *snail2* (neural crest), *hgg*, *gsc*, *ntl* (anterior notochord and polster), *isl1* (neuron precursors), *sox9b* (neural crest) and *shh* (neural tube floor plate) at 8 hpf, 10 hpf or 18 hpf was largely unchanged, except for subtle variations attributable to alterations in *grhl2b*-morphant size and shape (supplementary material Fig. S4F-N′). Taken together, our experiments suggested that specific early loss of *eng2a* in *grhl2b*-morphants led to defective MHB maintenance between 23 hpf and 28h pf, due to either increased cell death in the MHB region or to impaired regulatory feedback between *eng2a* and other MHB patterning genes.

To determine whether *grhl2a* may also function in MHB patterning, we injected embryos with a specific *grhl2a* ATG-blocking MO. As shown in supplementary material Fig. S5, knockdown of *grhl2a* led to a specific defect in body patterning, with severe shortening of the tail reminiscent of convergence-extension (CE) defects in zebrafish (Heisenberg et al., 2000), and consistent with the known roles of the *Grhl* family in regulating CE in the mouse (Ting et al., 2003). MHB development, however, was not significantly affected morphologically, and no loss of MHB markers was observed in these morphants. When *grhl2b* and *2a* were both downregulated through MO co-injection, a stronger trunk patterning defect was seen, concomitant with disrupted notochord formation. A slight defect was also seen in formation of the MHB basal constriction, suggesting that *grhl2a* may play a minor cooperative role with *grhl2b* in regulating MHB formation. An apparent sub-functionalisation of *Grhl2* in the zebrafish has occurred, whereby *grhl2a* primarily regulates axial patterning and *grhl2b* regulates MHB patterning and neural tube closure.

Loss of MHB markers is not due to apoptosis in *grhl2b* morphants

To evaluate the relationship between the increased cell death and loss of MHB markers in *grhl2b* morphants, we initially performed rescue experiments using MO-resistant murine *Grhl2* (*mGrhl2*) mRNA (Fig. 2A-E, Table 1). The abundant apoptotic cell death observed by bright-field microscopy and TUNEL staining in *grhl2b* morphants (51/81 embryos examined) was substantially reduced in *Grhl2*-rescued morphants (20/56 embryos examined; P=0.0017), emphasising the remarkable evolutionary conservation of function in the Grhl family. Importantly, the expression of MHB patterning markers, including *eng2a* and *pax2a* was also restored in *Grhl2*-rescued *grhl2b* morphants at 28 hpf (Fig. 2F-I; data not shown). These rescue experiments were subsequently repeated with a MO:resistant *grhl2b* mRNA, showing near-identical results for rescue of both apoptosis and MHB marker gene expression (data not shown). Despite this, the MHB folding defect was not rescued (Fig. 2B, inset), which we hypothesise to be due to the need for tightly controlled spatio-temporal expression of *grhl2b* for precise regulation of cellular polarity, consistent with known roles of *grh* in regulating cell polarity, and with previous work from our laboratory showing incomplete rescue of polarity-dependent phenotypes through simple restoration of gene expression (Caddy et al., 2010).

To determine whether prevention of apoptosis alone could also restore expression of MHB markers, the *grhl2b*-ATG blocking MO was injected into apoptosis-deficient, *p53*$^{-/-}$ fish (Berghmans et al., 2005) (Fig. 2J-O). Although apoptosis following MO-mediated *grhl2b* knockdown was substantially ameliorated in this line (Fig. 2J, inset), the number of fish exhibiting loss or reduction of MHB marker expression at 26 hpf was not significantly different between *p53*$^{-/-}$ fish [24/45; *eng2a* (96/12), *wnt1* (7/7), *pax2a* (7/18) and *her5* (4/8)] and wild-type fish [51/79; *eng2a* (16/24), *wnt1* (18/23), *pax2a* (6/14) and *her5* (10/18); P=0.219 by chi-square test; Fig. 2L-O; supplementary material Table S2). The defect in MHB folding was also not prevented. These findings indicate that *p53*-mediated neural apoptosis does not underpin MHB disruption in *grhl2b* morphants, and that the loss of MHB markers in these mutants may instead reflect perturbations of *eng2a* controlled homeostatic feedback mechanisms.

Eng2a rescues neural apoptosis and MHB marker loss in *grhl2b* morphants

The *Drosophila* orthologue of *eng2a*, *engrailed*, is a direct target of *grh* (Dynlacht et al., 1989; Attardi and Tjian, 1993), and the murine *eng2a* orthologue, engrailed 1, can be transcriptionally activated by the Grhl family (Wilanowski et al., 2002). Functionally, *En1* and *En2* prevent apoptosis of neural cells in the mouse midbrain (Sgado et al., 2006; Alavian et al., 2009), and vertebrate engrailed genes are crucial feedback molecules within the MHB maintenance cascade (Picker et al., 2002; Scholpp et al., 2003; Erickson et al., 2007). Furthermore, we observed elevated apoptosis in the MHB of *eng2a* morphants

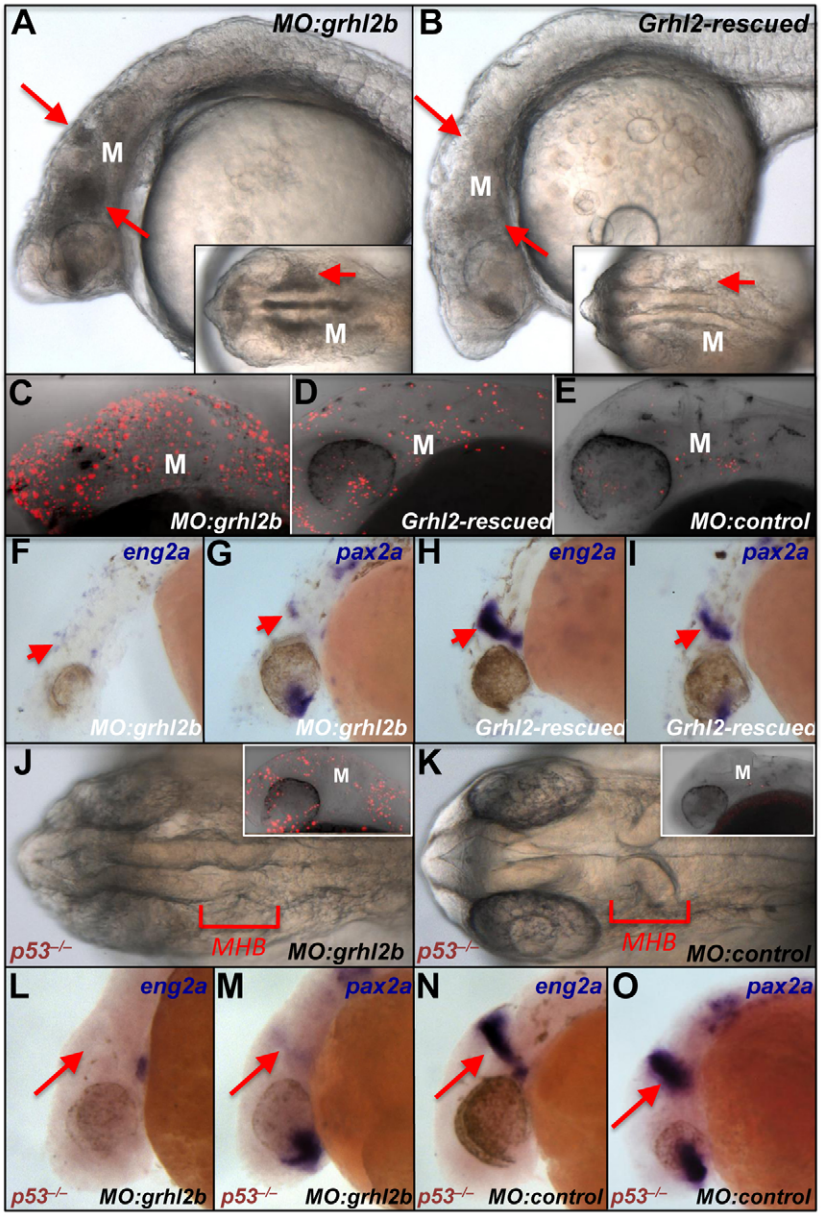

Fig. 2. Rescue of neural apoptosis and MHB marker loss in *grhl2b* morphants by mouse *Grhl2* mRNA. (**A-E**) Cell death rescue (arrows) demonstrated by bright-field microscopy (A,B, insets) and TUNEL staining (C-E) around the MHB region (M) of embryos sequentially injected with MO:*grhl2b* and either control *lacZ* mRNA (A,C) or mouse *Grhl2* mRNA (B,D). TUNEL staining reveals few apoptotic cells in an embryo injected with MO:*control* (E). (**F-I**) Rescue (arrows) of MHB marker expression (*eng2a, pax2a*) in embryos sequentially injected with MO:*grhl2b* and either *lacZ* mRNA (F,G) or mouse *Grhl2* mRNA (H,I). (**J-O**) Persistent defects in MHB folding (J,K) and marker expression (*eng2a, pax2a*) (L-O, arrows) in $p53^{-/-}$ fish injected with MO:*grhl2b* compared with MO:*control*. TUNEL assay confirms substantially reduced apoptosis in $p53^{-/-}$ fish injected with MO:*grhl2b* (J, inset; compare with C)

(data not shown). These data support the hypothesis that *grhl2b*-mediated loss of engrailed function leads to both neural apoptosis and loss of MHB markers. To test this, we injected *grhl2b* morphants with *eng2a* mRNA and examined the embryos by both bright-field microscopy (Fig. 3A-C) and TUNEL staining (Fig. 3D-F; Table 2). Of the non-rescued *grhl2b* morphants, 68/85 showed strong neural cell death, compared with 26/55 *eng2a*-rescued embryos ($P<0.001$), demonstrating a significant reduction in apoptosis. Crucially, expression of MHB markers was also restored in *eng2a*-rescued *grhl2b* morphants at the 26 hpf time point (Fig. 3G-I), but the MHB folding defect persisted (Fig. 3J,K). To confirm further the relationship between *eng2a* and *grhl2b*, we performed co-knockdown experiments, in which *grhl2b* and *eng2a* MOs were co-injected at sub-phenotype-causing doses (100 mM per MO). We observed loss of *pax2a* expression and increased cell death in approximately 50% of embryos (52/105), compared with 5-7% (4/72 and 8/112 for MO:*grhl2b* and MO:*eng2a*, respectively) when the MOs were injected individually (with MO:*control*) at the same concentration (Fig. 3L,M; Table 3). However, folding at the MHB still occurred in the co-injected embryos (Fig. 3M), suggesting that *eng2a* is crucial for *grhl2b*-dependent inhibition of apoptosis and maintenance of MHB markers, but not for morphogenesis. Previous

Table 1. Phenotypes observed following *Grhl2* rescue of MO-mediated loss of *grhl2b*

MO/mRNA injected	Number with neural cell death	Number with no neural cell death	Total	% rescue
MO:*grhl2b*+mRNA *lacZ*	51 (63.0%)	30 (37.0%)	81	–
MO:*grhl2b*+mRNA:*Grhl2*	20 (35.7%)	36 (64.3%)	56	43.30%

P-value (χ^2 test)=0.0017

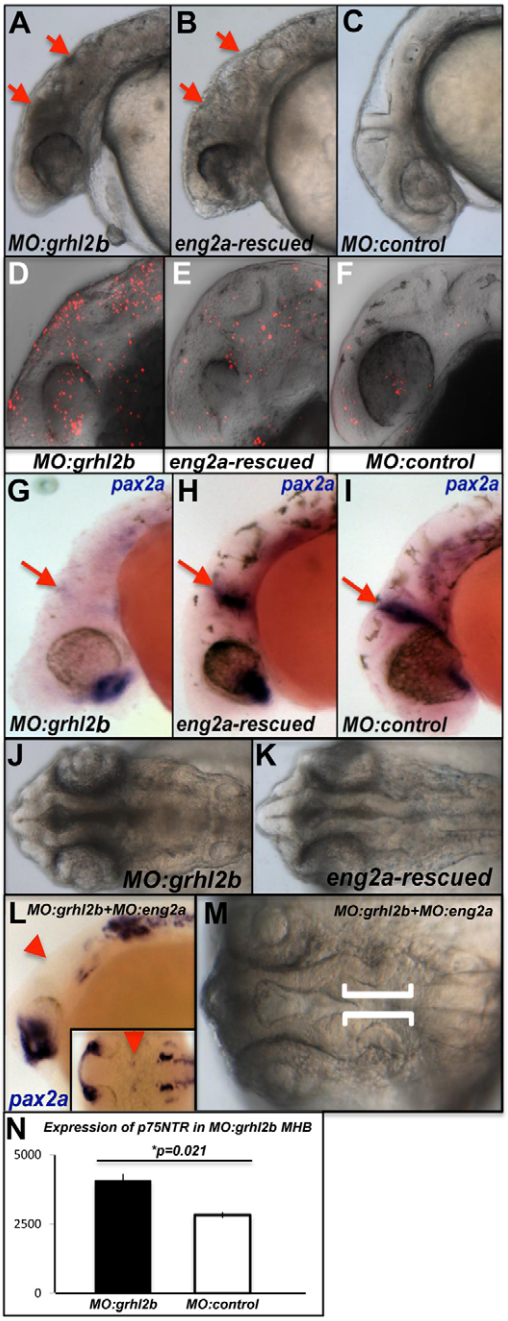

Fig. 3. Rescue of neural apoptosis and MHB marker loss in *grhl2b* morphants by *eng2a* mRNA. (**A-F**) Rescue of cell death (arrows) shown by bright-field microscopy (A-C) and TUNEL assay (D-F) in lateral views of 26 hpf embryos sequentially injected with MO:*grhl2b* and either *lacZ* mRNA (A,D) or *eng2a* mRNA (B,E). MO:*control* embryos injected with *lacZ* mRNA are shown (C,F). (**G-I**) Rescue of expression (arrows) of the MHB maintenance marker *pax2a* in 26 hpf embryos sequentially injected with MO:*grhl2b* and either *lacZ* (G) or *eng2a* (H). MO:*control* embryo injected with *lacZ* mRNA is shown (I). (**J**,**K**) MHB folding in *grhlb2* morphants (J) is not rescued by injection of *eng2a* mRNA (K). Injection of *lacZ* (J) as control. (**L**,**M**) Cooperativity between *grhl2b* and *eng2a* ATG-blocking MOs in inducing loss of *pax2a* expression and apoptosis (L, arrowhead; dorsal view, inset), but not MHB folding (brackets, M). Lateral views. (**N**) Q-RT-PCR analysis of MHBs extracted from *n*=3 MO:*grhl2b* 24 hpf morphants and MO:*control* embryos showing expression of p75NTR.

experiments had shown an upregulation of the pan-neurotrophin receptor p75NTR following disrupted engrailed signalling in mouse neurons (Alavian et al., 2009). Q-RT-PCR of the MHB regions of *grhl2b* morphants likewise showed a significant upregulation of this gene (P=0.021; Fig. 3N), consistent with increased apoptosis and loss of engrailed signalling in our model.

Direct regulation of *eng2a* by *grhl2b* in the MHB requires the two genes to be temporally and spatially co-expressed during development. To examine this we performed in situ hybridisation with *eng2a* and *grhl2b* probes on coronal sections of the MHB from embryos at 12 hpf (Fig. 4A,B). Although robust expression of *eng2a* was observed in all cells in this region, expression of *grhl2b* was observed strongly in only the neural ventral tissue. Close examination of these sections suggested that low levels of *grhl2b* expression may be evident more broadly throughout the MHB, and supporting this were recent data that also showed low levels of expression in the midbrain region (supplementary material Fig. S3H). To circumvent the problem of low sensitivity with in situ hybridisation, a common issue with analysis of transcription factors in general and with the *grhl* factors specifically (Janicke et al., 2010), we performed laser-capture microdissection (Fig. 4C,D) on coronal sections of MHB from wild-type embryos, and analysed expression of *grhl2b* and *eng2a* in the isolated cells by Q-RT-PCR. cDNA generated from one-cell embryos (pre-zygotic transcription) served as the negative control. Both *grhl2b* (Fig. 4E) and *eng2a* (Fig. 4F) were expressed in these cells, and given the near-ubiquitous *eng2a* expression in the dissected region (Fig. 4A), it is likely that these cells co-express both factors.

To confirm that *eng2a* is a direct transcriptional target of *grhl2b*, we examined the promoter of the *eng2a* gene for potential *grhl2b*-binding sites. The DNA consensus-binding site for all *grhl* family members is highly conserved from fly to human (Ting et al., 2005; Wilanowski et al., 2008; Caddy et al., 2010). Two putative binding sites were identified, at positions –1949 to –1942 (AACCAGTT) and –835 to –828 (AACCGTTT) relative to the transcriptional start site (TSS). As no antibodies are available to detect endogenous zebrafish *grhl2b*, we generated a C-terminal FLAG-tagged *grhl2b* construct (*grhl2b*-FLAG). This fusion construct was detectable by western blotting (Fig. 4G), and when overexpressed in one- to two-cell embryos, generated an identical eye defect phenotype to that observed with untagged *grhl2b* mRNA at 24 hpf (data not shown). ChIP on *grhl2b*-FLAG-expressing embryos demonstrated enrichment of both predicted sites within the *eng2a* promoter (Fig. 4H), indicating that *eng2a* is a direct target gene of *grhl2b*. Consistent with both our ChIP and expression data, in vivo reporter gene studies showed that MO-induced loss of *grhl2b* led to a sixfold reduction in expression from an *eng2a* promoter-*luciferase* reporter construct in embryos (Fig. 4I). Our data indicate that *grhl2b*-mediated regulation of *eng2a* is a novel, direct mechanism for regulating MHB patterning.

spec1 is a novel *grhl2b* target gene crucial for MHB morphogenesis

Both our results, and previously published data (Scholpp et al., 2004), suggest that *eng2a* is not required for establishing the characteristic neural tube morphology at the level of the MHB. Furthermore, recent evidence suggests that the molecular events that regulate MHB induction and patterning are distinct from those that regulate MHB morphogenesis (Gutzman et al., 2008) and ventricle development. To define the molecular mechanisms underpinning *grhl2b*-mediated regulation of MHB folding, we used the *Grhl* DNA consensus binding site to interrogate a customised

Table 2. Phenotypes observed following *eng2a* rescue of MO-mediated loss of *grhl2b*

MO/mRNA injected	Number with neural cell death	Number with no neural cell death	Total	% rescue
MO:*grhl2b*+mRNA *lacZ*	68 (80.0%)	17 (20.0%)	85	–
MO:*grhl2b*+mRNA:*eng2a*	26 (47.3%)	29 (52.7%)	55	40.90%

P-value (χ^2 test)=0.000057

dataset of genomic regions located within 10 kb of gene transcriptional start sites that are highly phylogenetically conserved. We have successfully used this approach previously to identify direct target genes of other *Grhl* factors (Caddy et al., 2010; Darido et al., 2011). One promising candidate target that emerged was *spec1* (small protein effector of *cdc42*, protein 1), also known as *cdc42se1* (*cdc42* small effector protein 1), a factor that binds to *cdc42* and influences actin accumulation in polarised T cells (Pirone et al., 2000; Ching et al., 2005; Ching et al., 2007). Data from migrating cells (which exhibit cell polarity) suggest that SPECs may generally be involved in *cdc42*-mediated polarity establishment in other cell types, besides lymphocytes, and may also regulate cell shape (Pirone et al., 2000).

The *spec1* promoter contained four putative *grhl2b*-binding sites within 2 kb of the TSS at positions: –1837 to –1830 (site 1, AACTAGTT), –714 to –707 (site 2, AACAGTTT), –291 to –284 (site 3, AACTGTTT) and –17 to –10 (site 4, AACCGGTG). ChIP assays using *grhl2b*-FLAG-expressing embryos demonstrated binding to three of these predicted sites (Fig. 5A), confirming that *spec1* is a direct target gene of *grhl2b*. ATG-MO-mediated knockdown of *spec1* led to complete abolition of MHB folding, phenocopying the non-folded MHB seen in *grhl2b* morphants (Fig. 5B,C). This phenotype was also seen with a splice-blocking-MO directed against the exon 1/intron 1 boundary of *spec1* (supplementary material Fig. S6A-C). Consistent with separate mechanisms being responsible for the loss of MHB patterning and MHB morphogenesis, *spec1* ATG or splice block morphants did not exhibit enhanced neural apoptosis (supplementary material Fig. S6D; data not shown) or loss of MHB-patterning markers (Fig. 5D,E; data not shown). *spec1* is maternally deposited and exhibits ubiquitous expression throughout zebrafish development (Thisse and Thisse, 2004) (data not shown), rendering in situ hybridisation of little value for examining *spec1* expression in *grhl2b* morphants. To counter this, we dissected out the MHB region from MO:*grhl2b*- and MO:*control*-injected embryos at 26 hpf and demonstrated reduced expression of *spec1* mRNA by Q-RT-PCR (Fig. 5F). To determine whether *grhl2b* and *spec1* functioned cooperatively in regulating MHB morphogenesis, we again performed co-knockdown experiments, in which *grhl2b* and *spec1* MOs were co-injected at sub-phenotype-causing doses (*MO:grhl2b* 100 mM, MO:*spec1* 125 mM). We observed severe folding (Fig. 5G) and ventricle formation (Fig. 5H) defects, which phenocopied the *grhl2b* knockdown, in ~40% of embryos (70/178), compared with 3-4% when the MOs were injected individually at the same concentration (6/154 for *grhl2b* and 7/168 for *spec1*, respectively; Table 4). Last, we reasoned that if *spec1* were a direct transcriptional target of *grhl2b* in the MHB, then expression of *spec1* mRNA should be increased following rescue of the *grhl2b* morphants with injection of *Grhl2* mRNA. Q-RT-PCR confirmed this hypothesis (Fig. 5I). As an additional control, *spec1* mRNA was also significantly increased in the MHB of wild-type embryos overexpressing *grhl2b* mRNA (Fig. 5J). Taken together, these data indicate that *grhl2b* directly regulates *spec1* to control MHB morphogenesis.

grhl2b acts with *fgf8* in MHB patterning and morphogenesis

Fgf8 functions as the main organising molecule of the isthmus, as it is required for development of both the tectum and cerebellum (Chi et al., 2003), and is sufficient to induce both structures in gain-of-function studies (Crossley et al., 1996; Martinez et al., 1999; Shamim et al., 1999). It also plays a central role in MHB maintenance, with *En1/2*, *Pax2/5* and *Fgf8* forming an inter-dependent feedback loop that is necessary for persistent expression of these genes (Nakamura, 2001). Consistent with studies in *Drosophila*, which show that the transcriptional activity of the Grh protein is enhanced by FGF signalling through a post-translational mechanism (Hemphala et al., 2003), we were unable to detect any change in either the timing or extent of *grhl2b* mRNA expression by either in situ hybridisation or Q-RT-PCR in the MHB region of *fgf8* morphants generated using an established MO (Araki and Brand, 2001) (supplementary material Fig. S7). We therefore examined whether *fgf8* and *grhl2b* interacted functionally by performing co-knockdown experiments with *grhl2b* and *fgf8* MOs co-injected at sub-phenotypic doses (100 mM each MO; Fig. 6A-L). Control (phenotypic) doses of MO:*fgf8* induced the expected *ace* phenotype, with concomitant apoptosis (Fig. 6A-C); MHB loss was also seen in 32% (11/34) of sub-phenotypically co-injected *grhl2b/fgf8* morphants (Fig. 6D-F). A further 56% (19/34) of these morphants (Fig. 6G-I) exhibited an even stronger phenotype, that of MHB loss and increased apoptosis, indicative of MO dose dependency. In total, 88% (30/34) of sub-phenotypically co-injected morphants displayed defective MHB/cerebellum development, compared with 7% of embryos injected with sub-phenotypic doses of MO:*fgf8*/MO:control (2/27; Fig. 6J-L; Table 5) or with 6% of embryos injected with sub-phenotypic doses of MO:*grhl2b*/MO:control (3/47; Table 5). These data indicate that *fgf8* and *grhl2b* operate within the same linear pathway to regulate MHB formation.

To determine whether these two genes could act cooperatively to regulate *eng2a* transcription, we performed sub-phenotypic injections of both MOs together with pGL3-*eng2a*-PROM, and assessed subsequent luciferase production. We found that *eng2a*-PROM-responsive luciferase production was significantly downregulated when both MOs were co-injected at sub-phenotypic doses, but not when either MO was injected at sub-phenotypic dose (together with MO:*control*), indicative of functional pathway cooperativity (Fig. 6M). Consistent with *grhl2b* being post-translationally, but not

Table 3. Phenotypes observed following MO-mediated loss of both *grhl2b* and *eng2a*

	Non-apposition of MHB folds	MHB loss and apoptosis	Wild type
MO:*grhl2b*+MO:control	1/72 (1.4%)	4/72 (5.5%)	67/72 (93.1%)
MO:*eng2a*+MO:control	2/112 (1.8%)	8/112 (7.1%)	102/112 (91.1%)
MO:*grhl2b*+MO:*eng2a*	16/105 (15.2%)	52/105 (49.5%)	37/105 (35.2%)

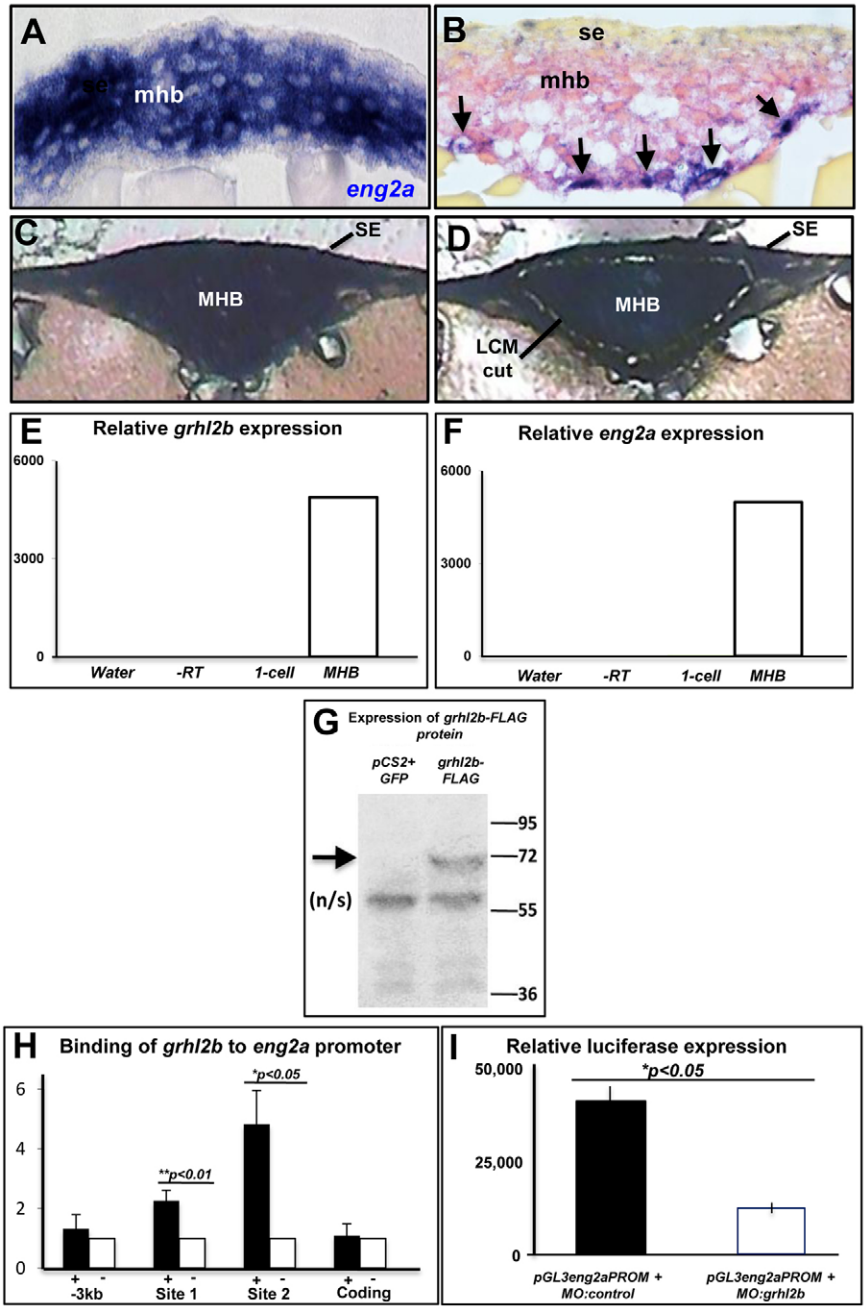

Fig. 4. *eng2a* is a direct target gene of *grhl2b* in the MHB. (**A**,**B**) High-powered coronal cross-sections, showing *eng2a* (A) and *grhl2b* (arrows) and *pax2a* (B) expression in the MHB in wild-type embryos at 12 hpf. mhb, midbrain-hindbrain boundary; se, surface ectoderm. (**C**,**D**) Coronal sections of MHB shown before laser capture microdissection (C) and highlighting the excised region (D). (**E**,**F**) Q-RT-PCR of *grhl2b* (E) and *eng2a* (F) from laser capture microdissection MHB tissue, relative to cDNA from pre-zygotic transcription-stage (one-cell) embryos, water and RT-negative controls. (**G**) Immunoblot of FLAG-tagged *grhl2b* (arrow) in cell extracts from HEK-293 cells transfected with pCS2+*grhl2b*-FLAG or the negative control (pCS2+GFP). n/s, non-specific band. (**H**) ChIP from embryos expressing FLAG-tagged *grhl2b* (+) or non-tagged *grhl2b* (–) using anti-FLAG antibody and primers for the two predicted *grhl2b*-binding sites in the *eng2a* promoter. Data are shown as the mean fold enrichment±s.e.m. (Q-RT-PCR) from two independent experiments performed with at least five embryos in each group. Negative control regions of the promoter or exon 1 ('–3 kb' and 'coding'. respectively) show no significant enrichment. (**I**) Reporter gene assay using a 3 kb region of the *eng2a* promoter linked to the *luciferase* gene (pGL3-*eng2a*-PROM) in 24 hpf embryos co-injected with either MO:*control* or MO:*grhl2b*. Data are shown as mean light units±s.e.m. from two independent experiments performed with a minimum of 40 embryos in each group.

transcriptionally, modified by *fgf8* signalling, enforced expression of wild-type *grhl2b* mRNA was incapable of rescuing the *ace* phenotype in MO:*fgf8*-injected embryos (supplementary material Fig. S7). As *eng2a* is already known to be lost in *fgf8*-null (*ace*) mutants (Reifers et al., 1998), we examined whether *spec1* was also downregulated in *fgf8*-deficient morphants, as predicted if loss of *fgf8* led to abrogated *grhl2b* function. We isolated regions of the neural tube at the level of the MHB in 18-19 hpf *fgf8*-morphants (pre-MHB morphogenesis), and Q-RT-PCR analysis showed that *spec1* expression was significantly downregulated ($P<0.005$) in *fgf8*-morphants at the formative stages of MHB morphogenesis (Fig. 6N). Taken together, our data, together with the previous experiments in *Drosophila* (Hemphala et al., 2003), suggest *grhl2b* and *fgf8* cooperate to regulate MHB patterning and morphogenesis in zebrafish, acting through *eng2a* and *spec1* (Fig. 6O). We hypothesise that *fgf8* may regulate *grhl2* post-transcriptionally, as is evident in the corresponding relationship in *Drosophila* (Hemphala et al., 2003), although proof of this hypothesis would require experiments to define and mutate the putative *fgf8*-induced phosphorylation sites in *grhl2b*.

DISCUSSION

In this paper, we provide evidence that the zebrafish transcription factor *grhl2b* plays key roles, putatively downstream of *fgf8*, in the morphogenesis and patterning of the mesencephalic-metencephalic regions of the developing vertebrate brain. This data expands on the known functions of the *Grhl* family in neuroblast specification, proliferation and apoptosis in *Drosophila* (Bray and Kafatos, 1991; Uv et al., 1997; Almeida and Bray, 2005; Cenci and Gould, 2005; Maurange et al., 2008), and neural tube morphogenesis in

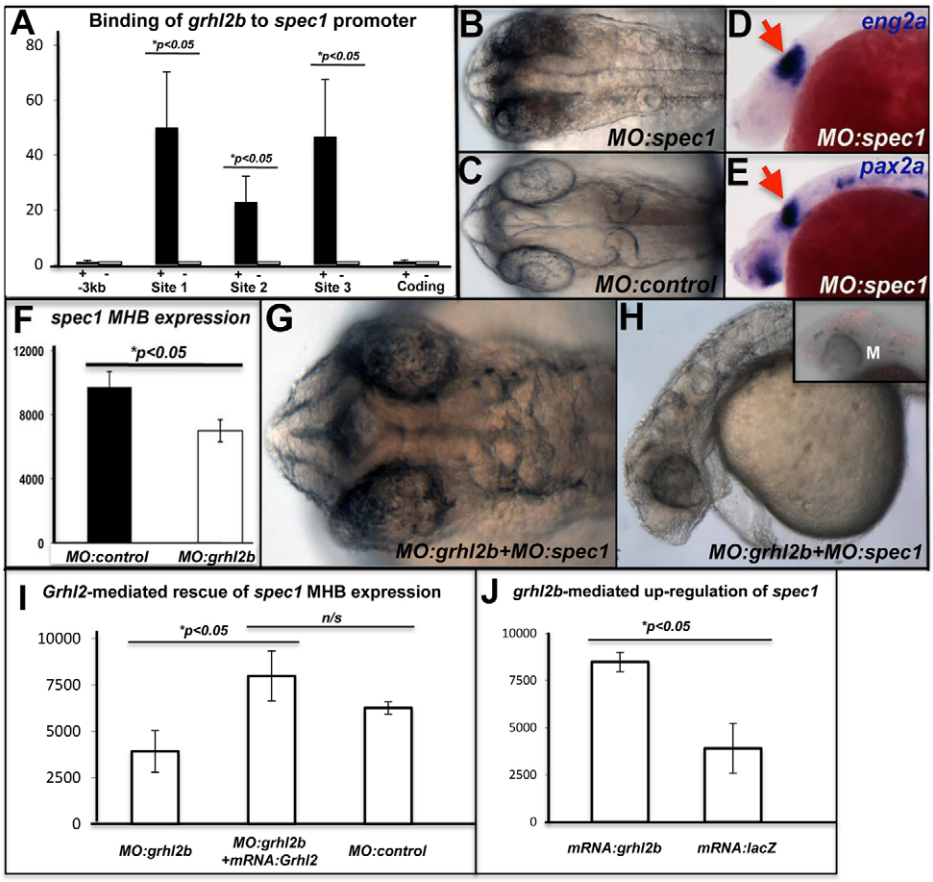

Fig. 5. *grhl2b* cooperates with a novel direct transcriptional target, *spec1*, to regulate MHB morphogenesis. (**A**) ChIP from embryos expressing FLAG-tagged *grhl2b* (+) or non-tagged *grhl2b* (–) using anti-FLAG antibody and primers to three predicted *grhl2b*-binding sites in the *spec1* promoter. Data are shown as the mean fold-enrichment±s.e.m. (Q-RT-PCR) from three independent experiments with at least five embryos per group. (**B**,**C**) Loss of MHB folding in *spec1* morphants at 26 hpf. (**D**,**E**) Expression of MHB markers (*eng2a*, *pax2a*, arrows) persists in *spec1* morphants at 26 hpf. (**F**) Q-RT-PCR of *spec1* expression in the MHB of *grhl2b* morphants. The MHB was dissected from five embryos per group, and the data are presented as the mean±s.d. (**G**,**H**) Cooperativity between *grhl2b* and *spec1* ATG-blocking MOs in inducing aberrant MHB folding (G, dorsal view), and mid/hindbrain ventricularisation (H, lateral view). (**I**,**J**) *spec1* mRNA expression at the MHB is restored following rescue of *grhl2b* morphants by injection of *Grhl2* mRNA (I), and is significantly upregulated in wild-type embryos overexpressing *grhl2b* mRNA (J).

mammals (Ting et al., 2003; Rifat et al., 2010), and highlights the evolutionary continuity of *grh/Grhl* gene function. We show that expression of MHB markers is initiated, but not maintained, in *grhl2b*-deficient embryos, and that this phenotype is not rescued by amelioration of apoptosis. Re-expression of *eng2a* in *grhl2b* morphants restores expression of *pax2a* and other MHB markers, and this, coupled with functional and biochemical data, identifies *eng2a* as a direct downstream target of *grhl2b*. However, the genetic interaction between *grhl2b* and *eng2a* does not influence MHB morphogenesis, suggesting that this process is separable from patterning. Consistent with this, we identified a second direct *grhl2b* target, *spec1*, which disrupts folding at the MHB, but does not alter expression of MHB markers.

The *grhl-eng* axis is conserved in evolution

Engrailed is an important factor for establishing and maintaining cellular compartments during *Drosophila* development (Hidalgo, 1996). Vertebrate homologues of *engrailed* also contribute to lineage-restricted compartments, as evidenced by the loss-of-function phenotypes in the mesencephalon (Wurst et al., 1994; Scholpp and Brand, 2001). As shown here in the fish, and previously in both fly and vertebrate systems, the *Grhl* factors are important regulators of *engrailed* expression (Dynlacht et al., 1989; Attardi and Tjian, 1993; Wilanowski et al., 2002), and expand the phylogenetically conserved mechanisms involved in regulation of the *engrailed* family. In the mouse, *Pax2*, *Pax5* and *Pax8*, homologues of the *Drosophila* pair-rule gene *paired* (a key transcriptional regulator of *engrailed*), are directly involved in maintenance of *En2* brain expression in a feedback loop (Song et al., 1996; Liu and Joyner, 2001). In the fish, the *paired* homologue *pax2a* is also necessary for normal *eng2* brain expression (Krauss et al., 1991). Taken together, these findings suggest that the genetic pathways involving regulation of the *engrailed* factors are highly conserved, despite evolving to control divergent developmental processes in flies and vertebrates.

grhl2b acts within the *fgf8* signalling pathway

Fgf8 signalling plays a central role in MHB positioning through coordinated expression of *otx2* and *gbx2* (Rhinn and Brand, 2001; Hidalgo-Sanchez et al., 2005). It is also pivotal for maintenance of the MHB, which is achieved via a complex series of feedback loops with factors including En1/2 and Pax2/5 (Joyner et al., 2000; Sato et al., 2004). Our data suggest that *grhl2b* is a crucial factor for *fgf8*-mediated induction of *En* expression. This effect does not occur at the level of transcription, as expression of *grhl2b* is not altered in *fgf8* morphants and enforced expression of *grhl2b* in *fgf8* morphants does not ameliorate the *ace* phenotype. However, the two genes act cooperatively, as shown by the high frequency of morphants with MHB defects observed when embryos are co-injected with sub-phenotypic doses of both *grhl2b* and *fgf8* MOs. Studies in *Drosophila* have shown that FGF signalling upregulates *grh* activity post-translationally (Hemphala et al., 2003). This is thought to be due to FGF-induced phosphorylation of *grh*, most probably by activated MAPK (ERK2), as *grh* is a known substrate

Table 4. Phenotype incidence following MO-mediated loss of both *grhl2b* and *spec1*

	Mis-folded MHB	Wild-type
MO:*grhl2b*+MO:control	6/154 (3.9%)	146/154 (96.1%)
MO:*spec1*+MO:control	7/168 (4.2%)	161/168 (95.8%)
MO:*grhl2b*+MO:*spec1*	70/178 (39.3%)	108/178 (60.7%)

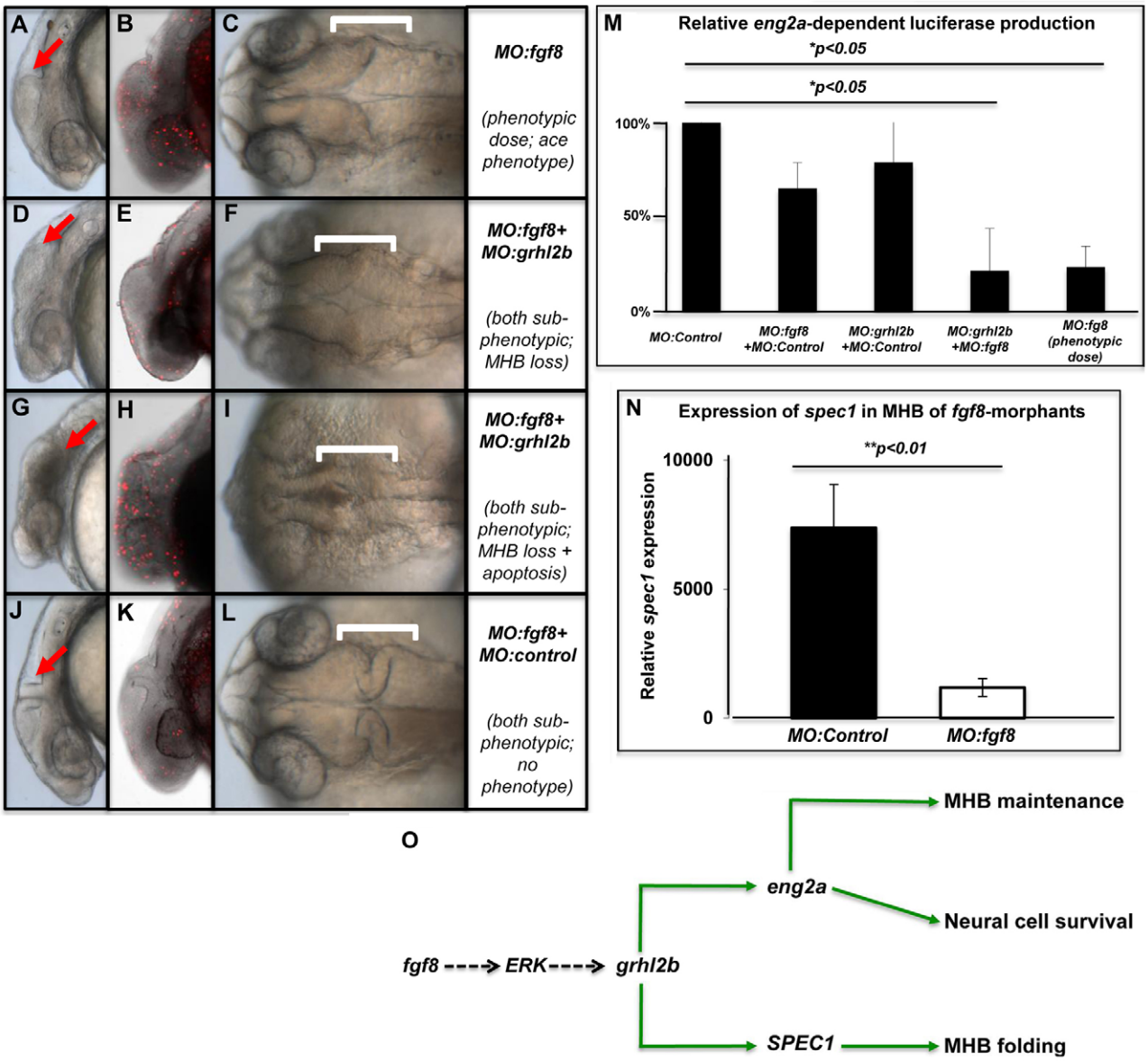

Fig. 6. *grhl2b* is a predicted downstream target of *fgf8* signalling. (**A-L**) Downregulation of *fgf8* causes loss of cerebellum and enhanced apoptosis (*ace* phenotype; A-C), a defect that is recapitulated when *fgf8* and *grhl2b* morpholinos are co-injected at individual sub-phenotypic doses (D-F). More severely affected *fgf8-grhl2b* double knockdown embryos display enhanced apoptosis and loss of MHB folding in a dose-dependent manner (G-I). No phenotypes or increased apoptosis are seen when *fgf8* and control morpholinos are co-injected at sub-phenotypic doses (J-L). Arrows and brackets in all panels show position of the MHB; B,E,H,K show TUNEL staining of the relevant phenotype. (**M**) Luciferase activity from pGL3-*eng2a*-PROM is significantly decreased following co-injection of sub-phenotypic doses of MO:*fgf8* and MO:*grhl2b,* but not when either MO is injected at sub-phenotypic doses together with MO:*control*. (**N**) *spec1* expression is lost in *fgf8* morphants at the formative stages of MHB morphogenesis. (**O**) Putative model of the predicted functional pathways of *fgf8/erk*-mediated regulation of *grhl2b* in MHB maintenance, neural apoptosis and MHB folding.

of this kinase (Liaw et al., 1995). Obvious parallels exist between these findings and the mechanism underpinning *fgf8* function in the MHB, which is also mediated through ERK signalling (Sato and Nakamura, 2004). Expression of a dominant-negative form of Ras induces repression of *Pax2/5* and *En1/2* expression (Sato and Nakamura, 2004), and these findings would be consistent with *grhl2b* functioning as the key intermediary in this pathway. Thus, post-translational activation of *grhl2b* by *fgf8* could ensure that the transcriptional activation of *eng2a* is confined to the MHB, and does not extend into adjacent regions, where *grhl2b* is also expressed.

Loss of *grhl2b* induces apoptosis

A prominent aspect of our *grhl2b* loss-of-function studies was apoptosis throughout the brain and nervous system, especially at the level of the MHB, which correlated with a loss of marker expression and MHB morphology. MHB apoptosis and marker loss is a feature of the fish mutant *ace*, which harbours a mutation in *fgf8* (Reifers et al., 1998; Jaszai et al., 2003), and in other models of MHB-marker loss (Brand et al., 1996; Chi et al., 2003). Our experiments also show MHB apoptosis following MO-mediated downregulation of *eng2a* (data not shown). We observed rescue of apoptosis in the *grhl2b* morphants with loss of *p53*, or with re-

Table 5. Phenotype incidence following MO-mediated loss of both *grhl2b* and *FGF8*

	Cerebellum loss	Mhb loss and apoptosis	Wild type
MO:grhl2b+MO:control	0/47 (0.0%)	3/47 (6.4%)	44/47 (93.6%)
MO:FGF8+MO:control	2/27 (7.4%)	0/27 (0.0%)	25/27 (92.6%)
MO:grhl2b+MO:FGF8	11/34 (32.3%)	19/34 (55.9%)	4/34 (11.8%)

expression of *grhl2b* and *eng2a*. This result does not implicate *eng2a* as the sole downstream effector of *grhl2b* for the prevention of apoptosis, however, as *Wnt1*, En and Pax genes display marked transcriptional interdependence. Despite the substantial rescue of apoptosis in the *grhl2b* morphants on a $p53^{-/-}$ genetic background, restoration of MHB marker expression was not observed, indicating that *grhl2b* provides instructive as well as anti-death signals. Consistent with this, rescue of *grhl2b*-morphants through the re-introduction of *eng2a* mRNA was both neuroprotective within the MHB, and restored the expression of MHB markers.

Defective neural tube folding in both mouse and fish *Grhl2*/*grhl2b* mutants

In addition to increased apoptosis and loss of MHB marker expression, we also observed defective MHB folding and ventricle development in the *grhl2b* morphants. This appears not to involve *eng2* as a downstream effector, despite both *grhl2b* and *fgf8* being implicated. Recent data suggests that MHB morphogenesis and subsequent ventricle inflation are regulated by non-patterning genes at the level of the MHB (Lowery and Sive, 2009). Zebrafish mutants *sleepy* and *grumpy* (laminin γ1 and β1, respectively) (Gutzman et al., 2008), *snakehead* (Atp1a1), and *nagie oko* (Mpp5) (Lowery and Sive, 2005) show various neural tube/MHB folding defects, and demarcate the process of MHB patterning from MHB morphogenesis. We have identified a further novel regulator of neural tube morphogenesis, *spec1*, which is a known regulator of the small RhoGTPase *cdc42* and a direct target of *grhl2b*. As *spec1* regulates cellular morphogenesis (Pirone et al., 2000), and changes in cell shape (in particular basal constriction) appear to be crucial for correct MHB folding in zebrafish (Gutzman et al., 2008), we propose that *spec1*-mediated regulation of *cdc42* is important for correct neural tube folding at the MHB. Consistent with this predicted mechanism, our data show that *spec1* has no effect in regulating neural cellular survival or MHB patterning. The involvement of *grhl2b* in both patterning and morphogenesis may explain why the phenotype of *Grhl2*-null mice is far more severe than most of the other MHB patterning mutants. A hallmark of the cranial defects in *Grhl2*-null mouse embryos is the absence of dorsolateral hinge point (DLHP) formation, which is central to neural plate folding in mammals (Rifat et al., 2010). Although the mechanism underpinning *Grhl2*-mediated DLHP formation is not known, a recent study suggests that defective formation of junctional complexes, mediated by E-cadherin and claudin 4 loss in *Grhl2*-deficient mice, may be responsible for failed neural tube closure (Werth et al., 2010).

Concluding remarks

Our study identifies two novel targets of *grhl2b* (*eng2a* and *spec1*), which regulate MHB patterning and morphogenesis. Through our use of combinatorial MO knockdown and mRNA rescue technologies, we have shown that these disparate processes are controlled by *grhl2b* through direct regulation of two different transcriptional targets. As the full spectrum of *grhl2b* target genes remains to be elucidated, future work will further refine these, and other genetic pathways influenced by *grhl2b* in neurulation.

Acknowledgements

We thank Dr Heather Verkade, Prof. Michael Brand and Dr Andrew Waszkiewicz for providing in-situ hybridisation probes and/or full-length cDNA plasmids; Dr Quan Zhao and Dr Chris Slape for assistance with ChIP assays; Mr Cameron Nowell for assistance with confocal microscopy; Dr Matthew McCormack for assistance with statistical analysis; and Dr Stewart Fabb, Dr Andrew Badrock and John Hayman for technical assistance.

Funding

S.M.J. is a Principal Research Fellow of the Australian National Health and Medical Research Council (NHMRC). The work was partially supported by project grants from the NHMRC [435112 and 544304], and by a grant from the March of Dimes Foundation [6-FY07-293].

Competing interests statement

The authors declare no competing financial interests.

Supplementary material

Supplementary material available online at
http://dev.biologists.org/lookup/suppl/doi:10.1242/dev.066522/-/DC1

References

Alavian, K. N., Sgado, P., Alberi, L., Subramaniam, S. and Simon, H. H. (2009). Elevated P75NTR expression causes death of engrailed-deficient midbrain dopaminergic neurons by Erk1/2 suppression. *Neural Dev.* **4**, 11.

Alcaraz-Perez, F., Mulero, V. and Cayuela, M. L. (2008). Application of the dual-luciferase reporter assay to the analysis of promoter activity in Zebrafish embryos. *BMC Biotechnol.* **8**, 81.

Almeida, M. S. and Bray, S. J. (2005). Regulation of post-embryonic neuroblasts by Drosophila Grainyhead. *Mech. Dev.* **122**, 1282-1293.

Araki, I. and Brand, M. (2001). Morpholino-induced knockdown of Fgf8 efficiently phenocopies the acerebellar (ace) phenotype. *Genesis* **30**, 157-159.

Attardi, L. D. and Tjian, R. (1993). Drosophila tissue-specific transcription factor NTF-1 contains a novel isoleucine-rich activation motif. *Genes Dev.* **7**, 1341-1353.

Berghmans, S., Murphey, R. D., Wienholds, E., Neuberg, D., Kutok, J. L., Fletcher, C. D., Morris, J. P., Liu, T. X., Schulte-Merker, S., Kanki, J. P. et al. (2005). tp53 mutant zebrafish develop malignant peripheral nerve sheath tumors. *Proc. Natl. Acad. Sci. USA* **102**, 407-412.

Brand, M., Heisenberg, C. P., Jiang, Y. J., Beuchle, D., Lun, K., Furutani-Seiki, M., Granato, M., Haffter, P., Hammerschmidt, M., Kane, D. A. et al. (1996). Mutations in zebrafish genes affecting the formation of the boundary between midbrain and hindbrain. *Development* **123**, 179-190.

Bray, S. J. and Kafatos, F. C. (1991). Developmental function of Elf-1: an essential transcription factor during embryogenesis in Drosophila. *Genes Dev.* **5**, 1672-1683.

Caddy, J., Wilanowski, T., Darido, C., Dworkin, S., Ting, S. B., Zhao, Q., Rank, G., Auden, A., Srivastava, S., Papenfuss, T. A. et al. (2010). Epidermal wound repair is regulated by the planar cell polarity signaling pathway. *Dev. Cell* **19**, 138-147.

Cenci, C. and Gould, A. P. (2005). Drosophila Grainyhead specifies late programmes of neural proliferation by regulating the mitotic activity and Hox-dependent apoptosis of neuroblasts. *Development* **132**, 3835-3845.

Chi, C. L., Martinez, S., Wurst, W. and Martin, G. R. (2003). The isthmic organizer signal FGF8 is required for cell survival in the prospective midbrain and cerebellum. *Development* **130**, 2633-2644.

Ching, K. H., Kisailus, A. E. and Burbelo, P. D. (2005). The role of SPECs, small Cdc42-binding proteins, in F-actin accumulation at the immunological synapse. *J. Biol. Chem.* **280**, 23660-23667.

Ching, K. H., Kisailus, A. E. and Burbelo, P. D. (2007). Biochemical characterization of distinct regions of SPEC molecules and their role in phagocytosis. *Exp. Cell Res.* **313**, 10-21.

Clark, K. J., Balciunas, D., Pogoda, H.-M., Ding, Y., Westcot, S. E., Bedell, V. M., Greenwood, T. M., Urban, M. D., Skuster, K. J., Petzold, A. M. et al. (2011). In vivo protein trapping produces a functional expression codex of the vertebrate proteome. *Nat. Methods* **8**, 506-512.

Crossley, P. H., Martinez, S. and Martin, G. R. (1996). Midbrain development induced by FGF8 in the chick embryo. *Nature* **380**, 66-68.

Dahl, J. A. and Collas, P. (2008). A rapid micro chromatin immunoprecipitation assay (microChIP). *Nat. Protoc.* **3**, 1032-1045.
Darido, C., Georgy, S. R., Wilanowski, T., Dworkin, S., Auden, A., Zhao, Q., Rank, G., Srivastava, S., Finlay, M. J., Papenfuss, A. T. et al. (2011). Targeting of the novel tumor suppressor GRHL3 by a miR-21-dependent proto-oncogenic network results in PTEN loss and tumorigenesis. *Cancer Cell* **20**, 635-648.
Dworkin, S., Heath, J. K., de Jong-Curtain, T. A., Hogan, B. M., Lieschke, G. J., Malaterre, J., Ramsay, R. G. and Mantamadiotis, T. (2007). CREB activity modulates neural cell proliferation, midbrain-hindbrain organization and patterning in zebrafish. *Dev. Biol.* **307**, 127-141.
Dynlacht, B. D., Attardi, L. D., Admon, A., Freeman, M. and Tjian, R. (1989). Functional analysis of NTF-1, a developmentally regulated Drosophila transcription factor that binds neuronal cis elements. *Genes Dev.* **3**, 1677-1688.
Erickson, T., Scholpp, S., Brand, M., Moens, C. B. and Waskiewicz, A. J. (2007). Pbx proteins cooperate with Engrailed to pattern the midbrain-hindbrain and diencephalic-mesencephalic boundaries. *Dev. Biol.* **301**, 504-517.
Gutzman, J. H., Graeden, E. G., Lowery, L. A., Holley, H. S. and Sive, H. (2008). Formation of the zebrafish midbrain-hindbrain boundary constriction requires laminin-dependent basal constriction. *Mech. Dev.* **125**, 974-983.
Han, Y., Mu, Y., Li, X., Xu, P., Tong, J., Liu, Z., Ma, T., Zeng, G., Yang, S., Du, J. et al. (2011). Grhl2 deficiency impairs otic development and hearing ability in a zebrafish model of the progressive dominant hearing loss DFNA28. *Hum. Mol. Genet.* **20**, 3213-3226.
Hanks, M. C., Loomis, C. A., Harris, E., Tong, C. X., Anson-Cartwright, L., Auerbach, A. and Joyner, A. (1998). Drosophila engrailed can substitute for mouse Engrailed1 function in mid-hindbrain, but not limb development. *Development* **125**, 4521-4530.
Heisenberg, C. P., Tada, M., Rauch, G. J., Saúde, L., Concha, M. L., Geisler, R., Stemple, D. L., Smith, J. C. and Wilson, S. W. (2000). Silberblick/Wnt11 mediates convergent extension movements during zebrafish gastrulation. *Nature* **405**, 76-81.
Hemphala, J., Uv, A., Cantera, R., Bray, S. and Samakovlis, C. (2003). Grainy head controls apical membrane growth and tube elongation in response to Branchless/FGF signalling. *Development* **130**, 249-258.
Hidalgo, A. (1996). The roles of engrailed. *Trends Genet.* **12**, 1-4.
Hidalgo-Sanchez, M., Millet, S., Bloch-Gallego, E. and Alvarado-Mallart, R. M. (2005). Specification of the meso-isthmo-cerebellar region: the Otx2/Gbx2 boundary. *Brain Res. Brain Res. Rev.* **49**, 134-149.
Janicke, M., Renisch, B. and Hammerschmidt, M. (2010). Zebrafish grainyhead-like1 is a common marker of different non-keratinocyte epidermal cell lineages, which segregate from each other in a Foxi3-dependent manner. *Int. J. Dev. Biol.* **54**, 837-850.
Jaszai, J., Reifers, F., Picker, A., Langenberg, T. and Brand, M. (2003). Isthmus-to-midbrain transformation in the absence of midbrain-hindbrain organizer activity. *Development* **130**, 6611-6623.
Joyner, A. L. (1996). Engrailed, Wnt and Pax genes regulate midbrain-hindbrain development. *Trends Genet.* **12**, 15-20.
Joyner, A. L., Herrup, K., Auerbach, B. A., Davis, C. A. and Rossant, J. (1991). Subtle cerebellar phenotype in mice homozygous for a targeted deletion of the En-2 homeobox. *Science* **251**, 1239-1243.
Joyner, A. L., Liu, A. and Millet, S. (2000). Otx2, Gbx2 and Fgf8 interact to position and maintain a mid-hindbrain organizer. *Curr. Opin. Cell Biol.* **12**, 736-741.
Krauss, S., Johansen, T., Korzh, V. and Fjose, A. (1991). Expression of the zebrafish paired box gene pax[zf-b] during early neurogenesis. *Development* **113**, 1193-1206.
Liaw, G. J., Rudolph, K. M., Huang, J. D., Dubnicoff, T., Courey, A. J. and Lengyel, J. A. (1995). The torso response element binds GAGA and NTF-1/Elf-1, and regulates tailless by relief of repression. *Genes Dev.* **9**, 3163-3176.
Liu, A. and Joyner, A. L. (2001). EN and GBX2 play essential roles downstream of FGF8 in patterning the mouse mid/hindbrain region. *Development* **128**, 181-191.
Lowery, L. A. and Sive, H. (2005). Initial formation of zebrafish brain ventricles occurs independently of circulation and requires the nagie oko and snakehead/atp1a1a.1 gene products. *Development* **132**, 2057-2067.
Lowery, L. A. and Sive, H. (2009). Totally tubular: the mystery behind function and origin of the brain ventricular system. *BioEssays* **31**, 446-458.
Lun, K. and Brand, M. (1998). A series of no isthmus (noi) alleles of the zebrafish pax2.1 gene reveals multiple signaling events in development of the midbrain-hindbrain boundary. *Development* **125**, 3049-3062.
Martinez, S. (2001). The isthmic organizer and brain regionalization. *Int. J. Dev. Biol.* **45**, 367-371.
Martinez, S., Crossley, P. H., Cobos, I., Rubenstein, J. L. and Martin, G. R. (1999). FGF8 induces formation of an ectopic isthmic organizer and isthmocerebellar development via a repressive effect on Otx2 expression. *Development* **126**, 1189-1200.
Maurange, C., Cheng, L. and Gould, A. P. (2008). Temporal transcription factors and their targets schedule the end of neural proliferation in Drosophila. *Cell* **133**, 891-902.
Nakamura, H. (2001). Regionalization of the optic tectum: combinations of gene expression that define the tectum. *Trends Neurosci.* **24**, 32-39.
Picker, A., Scholpp, S., Bohli, H., Takeda, H. and Brand, M. (2002). A novel positive transcriptional feedback loop in midbrain-hindbrain boundary development is revealed through analysis of the zebrafish pax2.1 promoter in transgenic lines. *Development* **129**, 3227-3239.
Pirone, D. M., Fukuhara, S., Gutkind, J. S. and Burbelo, P. D. (2000). SPECs, small binding proteins for Cdc42. *J. Biol. Chem.* **275**, 22650-22656.
Reifers, F., Bohli, H., Walsh, E. C., Crossley, P. H., Stainier, D. Y. and Brand, M. (1998). Fgf8 is mutated in zebrafish acerebellar (ace) mutants and is required for maintenance of midbrain-hindbrain boundary development and somitogenesis. *Development* **125**, 2381-2395.
Rhinn, M. and Brand, M. (2001). The midbrain-hindbrain boundary organizer. *Curr. Opin. Neurobiol.* **11**, 34-42.
Rhinn, M., Lun, K., Ahrendt, R., Geffarth, M. and Brand, M. (2009). Zebrafish gbx1 refines the midbrain-hindbrain boundary border and mediates the Wnt8 posteriorization signal. *Neural Dev.* **4**, 12.
Rifat, Y., Parekh, V., Wilanowski, T., Hislop, N. R., Auden, A., Ting, S. B., Cunningham, J. M. and Jane, S. M. (2010a). Regional neural tube closure defined by the Grainy head-like transcription factors. *Dev. Biol.* **345**, 237-245.
Sato, T. and Nakamura, H. (2004). The Fgf8 signal causes cerebellar differentiation by activating the Ras-ERK signaling pathway. *Development* **131**, 4275-4285.
Sato, T., Joyner, A. L. and Nakamura, H. (2004). How does Fgf signaling from the isthmic organizer induce midbrain and cerebellum development? *Dev. Growth Differ.* **46**, 487-494.
Scholpp, S. and Brand, M. (2001). Morpholino-induced knockdown of zebrafish engrailed genes eng2 and eng3 reveals redundant and unique functions in midbrain-hindbrain boundary development. *Genesis* **30**, 129-133.
Scholpp, S., Groth, C., Lohs, C., Lardelli, M. and Brand, M. (2004). Zebrafish fgfr1 is a member of the fgf8 synexpression group and is required for fgf8 signalling at the midbrain-hindbrain boundary. *Dev. Genes Evol.* **214**, 285-295.
Scholpp, S., Lohs, C. and Brand, M. (2003). Engrailed and Fgf8 act synergistically to maintain the boundary between diencephalon and mesencephalon. *Development* **130**, 4881-4893.
Sgado, P., Alberi, L., Gherbassi, D., Galasso, S. L., Ramakers, G. M., Alavian, K. N., Smidt, M. P., Dyck, R. H. and Simon, H. H. (2006). Slow progressive degeneration of nigral dopaminergic neurons in postnatal Engrailed mutant mice. *Proc. Natl. Acad. Sci. USA* **103**, 15242-15247.
Shamim, H., Mahmood, R., Logan, C., Doherty, P., Lumsden, A. and Mason, I. (1999). Sequential roles for Fgf4, En1 and Fgf8 in specification and regionalisation of the midbrain. *Development* **126**, 945-959.
Song, D. L., Chalepakis, G., Gruss, P. and Joyner, A. L. (1996). Two Pax-binding sites are required for early embryonic brain expression of an Engrailed-2 transgene. *Development* **122**, 627-635.
Thisse, B. and Thisse, C. (2004). Fast release clones: a high throughput expression analysis. ZFIN Direct Data Submission (http://zfin.org).
Ting, S. B., Wilanowski, T., Auden, A., Hall, M., Voss, A. K., Thomas, T., Parekh, V., Cunningham, J. M. and Jane, S. M. (2003). Inositol- and folate-resistant neural tube defects in mice lacking the epithelial-specific factor Grhl-3. *Nat. Med.* **9**, 1513-1519.
Ting, S. B., Caddy, J., Hislop, N., Wilanowski, T., Auden, A., Zhao, L. L., Ellis, S., Kaur, P., Uchida, Y., Holleran, W. M. et al. (2005). A homolog of Drosophila grainy head is essential for epidermal integrity in mice. *Science* **308**, 411-413.
Turner, D. L. and Weintraub, H. (1994). Expression of achaete-scute homolog 3 in Xenopus embryos converts ectodermal cells to a neural fate. *Genes Dev.* **8**, 1434-1447.
Uv, A. E., Harrison, E. J. and Bray, S. J. (1997). Tissue-specific splicing and functions of the Drosophila transcription factor Grainyhead. *Mol. Cell. Biol.* **17**, 6727-6735.
Werth, M., Walentin, K., Aue, A., Schonheit, J., Wuebken, A., Pode-Shakked, N., Vilianovitch, L., Erdmann, B., Dekel, B., Bader, M. et al. (2010). The transcription factor grainyhead-like 2 regulates the molecular composition of the epithelial apical junctional complex. *Development* **137**, 3835-3845.
Wilanowski, T., Tuckfield, A., Cerruti, L., O'Connell, S., Saint, R., Parekh, V., Tao, J., Cunningham, J. M. and Jane, S. M. (2002). A highly conserved novel family of mammalian developmental transcription factors related to Drosophila grainyhead. *Mech. Dev.* **114**, 37-50.
Wilanowski, T., Caddy, J., Ting, S. B., Hislop, N. R., Cerruti, L., Auden, A., Zhao, L. L., Asquith, S., Ellis, S., Sinclair, R. et al. (2008). Perturbed desmosomal cadherin expression in grainy head-like 1-null mice. *EMBO J.* **27**, 886-897.
Wurst, W. and Bally-Cuif, L. (2001). Neural plate patterning: upstream and downstream of the isthmic organizer. *Nat. Rev. Neurosci.* **2**, 99-108.
Wurst, W., Auerbach, A. B. and Joyner, A. L. (1994). Multiple developmental defects in Engrailed-1 mutant mice: an early mid-hindbrain deletion and patterning defects in forelimbs and sternum. *Development* **120**, 2065-2075.